Mon. Not. R. Astron. Soc. **277**, 767–776 (1995)

Water vapour in cool dwarf stars

Hugh R.A. Jones,[1] Andrew J. Longmore,[2] France Allard,[3] Peter H. Hauschildt,[4] Steven Miller[5] and Jonathan Tennyson[5]

[1]*Institute for Astronomy, University of Edinburgh, Blackford Hill, Edinburgh EH9 3HJ*
[2]*Royal Observatory, Blackford Hill, Edinburgh EH9 3HJ*
[3]*Department of Geophysics and Astronomy, University of British Columbia, Vancouver V6T 1Z4, Canada*
[4]*Department of Physics and Astronomy, Arizona State University, Box 871504, Tempe, AZ 85287-1504, USA*
[5]*Department of Physics and Astronomy, University College London, Gower Street, London WC1E 6BT*

Accepted 1995 May 19. Received 1995 May 9; in original form 1995 March 27

ABSTRACT

We present comparisons which show good agreement between observed and synthetic spectra for water vapour transitions in a range of M dwarfs. The observations were made from 2.85 to 3.40 μm where water vapour transitions are strong in cool stars but relatively weak in the Earth's atmosphere, allowing reliable observations to be made. The synthetic spectra were computed using a stellar atmosphere code and include preliminary *ab initio* calculations for ro-vibrational bands up to $J = 30$. Synthetic spectra indicate that changes in metallicity and gravity have a small effect on the strength of the observed water bands whereas temperature changes produce large differences in strength. Formally, we find similar effective temperatures to those found in previous work. However, since the molecular opacity at the peak of the flux distribution is not well determined, uncertainties in the model atmosphere structure and the effective temperature scale remain.

Detailed line profiles can be modelled for atomic lines because their damping constants are known, but they are not known for molecular transitions. Atomic lines computed with Voigt profiles and Van der Waals pressure broadening give an averaged full width half maximum of around 50 km s^{-1}. For the observed water vapour transitions to match this generation of synthetic spectra we use Gaussian profiles with a full width half maximum of 2 km s^{-1} to model the pressure broadening of water vapour transitions. Examination of the model structure indicates that water vapour lines are formed relatively high in the photosphere at pressures about an order of magnitude lower than those of atomic lines. These results strongly suggest that water vapour transitions are not pressure broadened sufficiently to overlap; as previously assumed when modelling molecular transitions in cool dwarfs using the Just Overlapping Line Approximation. The inferred lack of pressure broadening allows flux to escape between water lines, even within a region of strong water vapour absorption, and leads to weaker water band strengths. We demonstrate that this result is likely to explain much of the past discrepancy between observed and theoretical spectral energy distributions for M dwarfs.

Key words: molecular data – stars: late-type – stars: low-mass, brown dwarfs – infrared: stars.

1 INTRODUCTION

Molecular absorption bands have been used as a diagnostic of spectral type since the 1860s. TiO was first identified as the dominant feature in optical spectra of cool giants (Fowler 1904). Over the last 30 years, diatomic molecules have been included in detailed calculations of stellar opacity. The success of these studies and a desire to understand cooler objects mean that attention is starting to focus on the incorporation of accurate data for triatomic molecules. The most important is water.

M dwarfs are the dominant stellar population in the Galaxy. They emit the bulk of their radiation at near-infrared wavelengths where water vapour is the principal source of opacity in their atmospheres. The shape of the water absorption bands means that their energy distributions do not

resemble the blackbody curves which are shown by hotter stars across the near-infrared. The lack of accurate water vapour data available for inclusion in model atmosphere codes has meant that synthetic and observed spectra do not match well enough for the derived parameters to be trusted (e.g. Tinney, Mould & Reid 1993). This has led to a number of different empirical techniques to determine the effective temperatures of M dwarfs. These have yielded a wide range of effective temperature scales. A model atmosphere calculation that properly accounts for water vapour should yield an unambiguous effective temperature scale for M dwarfs. Over the last ten years many papers have discussed the discovery of candidate brown dwarfs. Yet without an accurate effective temperature scale for M dwarfs it has not been possible to distinguish whether they are brown dwarfs or late-type M dwarfs.

For effective temperatures applicable to cool star atmospheres (<4000 K) it is necessary to cover the band origins of water up to 30 000 cm^{-1} and angular momentum states up to $J = 55$ (30 000 cm^{-1}) above the ground state. Such a calculation requires a significant investment of time on the most powerful computers currently available. Before undertaking such a large investment of computer time a preliminary calculation of 8.4×10^6 transitions including states up to $J = 30$ was made (Schryber, Miller & Tennyson 1995). This preliminary water line list has been incorporated in the PHOENIX model atmosphere code (Hauschildt 1991; Allard et al. 1994; Hauschildt et al. 1994, 1995). The following work compares the latest version of PHOENIX including the preliminary water line list with high-quality observations of stellar water vapour.

The preponderance of water vapour in the Earth's atmosphere makes it very difficult to observe its spectral signature in stars. At near-infrared wavelengths, where cool stars emit most of their flux, the strongest water vapour absorption band for cool stars is centred around 2.65 μm where the atmosphere is opaque. However, all molecular bands become narrower towards lower effective temperatures as fewer of the higher ro-vibrational states are occupied. Because M dwarfs are an order of magnitude hotter than the atmosphere, ground-based observations can be made in the wings of this band. Transitions of a weaker band at 3.17 μm are also observable. We considered that the 2.65- and 3.17-μm bands were more appropriate for this part of our study than the bands at 1.4 and 1.7 μm because they are affected less by the low-energy cut-off of the calculations.

The observations and data reduction procedures are reported in Section 2. The *ab initio* calculations are discussed in Section 3. Comparisons with other water vapour opacity datasets are made in Section 4. The model atmospheres are presented in Section 5. Section 6 compares the observed and synthetic spectra. Future work is highlighted in Section 7.

2 OBSERVATIONS

We observed a range of M dwarfs – VB10 (M8V), GL406 (M6V), GL699 (M3.5V) and GL411 (M2V). They were chosen because they have been the subject of many previous studies of M dwarfs (e.g. Jones et al. 1994) and because they form a sample whose space motions and colours indicate that they cover a wide range of effective temperature, but probably a narrow range in metallicity.

The observations were made on the nights of 1993 April 21–23 with the Cooled Grating Spectrometer 4 (CGS4, Mountain et al. 1990) on the UK Infrared Telescope on Mauna Kea, Hawaii. CGS4 used a 58 × 62 InSb array which was moved in the focal plane in order to over-sample the spectrum. Comparison sky spectra were obtained by nodding the telescope so that the object was measured successively in two rows of the array, separated by 30 arcsec (10 rows on the array).

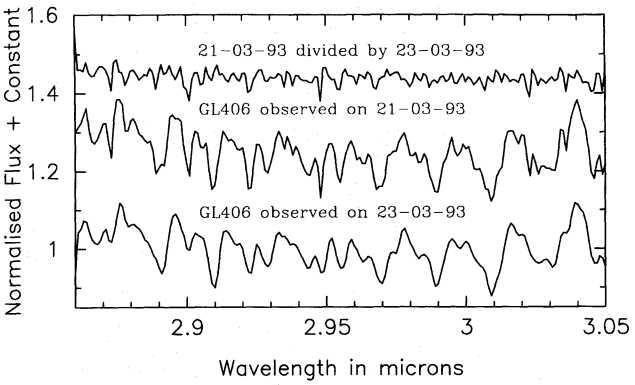

Figure 1. To check the reproducibility of the spectra in this little-used spectral region, a number of the observations were repeated. Observations of GL406 at the same grating position taken on 1993 April 21 and 23 are shown. Both observations are normalized to have the same mean value of one and then offset by the addition of 0.25; in the upper part, the normalized observations have been divided by one another and the result offset by the addition of 0.5.

The 150 line mm^{-1} grating was used with central grating wavelengths of 2.94, 3.12 and 3.3 μm. These grating positions enable complete coverage from 2.86 to 3.4 μm at a resolution of around 1000. Observations were also made with the 75 line mm^{-1} grating at a central wavelength position of 3.12 μm, giving a resolution of around 500 and covering 2.94–3.34 μm. This was done to check the reproducibility of features in a little-used spectral region and to ensure that accurate spectral overlaps were made when joining different spectral regions together. The high thermal background in the 2.8–3.4 μm region meant that a number of short integrations (0.5–2.0 s) were made and coadded together. For the faintest object, VB10, total on-chip integration times at each grating position were around 1 h; for the brighter objects, GL411, GL699 and GL406, they were around 30 min.

2.1 Data reduction

In the reduction of spectra, the same procedures as in Jones et al. (1994) have been followed. All observations were calibrated by taking short exposures of an argon lamp in the CGS4 calibration unit. This procedure is typically accurate to $0.1\Delta\lambda$ (Puxley, Ramsay & Beard 1992), where $\Delta\lambda$ is the instrumental resolution. The observed spectra were taken in a region where there are about half as many arc lines as normally available and so a wavelength calibration error of $0.2\Delta\lambda$ is more realistic. The wavelength calibration was checked by comparing the wavelength scale from the 75 line mm^{-1} grating with that from the 150 line mm^{-1} grating. They were found to agree to within $0.1\Delta\lambda$ of those from the 75 line mm^{-1} grating.

Stars from The Bright Star Catalogue (Hoffleit & Jaschek 1982) were used as standards to remove the effects of atmospheric absorption; these are given in Table 1. We found them

Table 1. The target objects were corrected for atmospheric transmission and flux calibrated using the standards listed above. The spectral types are from Hoffleit & Jaschek (1982); their effective temperatures were obtained from the $T_{\rm eff}$ – spectral type and colour relations of Johnson (1966) and Schlosser, Schmidt-Kaler & Milone (1991).

Object	Standards	Types	$T_{\rm eff}$ (K)
GL411	BS4345, BS4294	G0V, A5III	6030, 8100
GL699	BS6797, BS5304	F5V, F9IV	6440, 6060
GL406	BS4294, BS4386, BS4345	A5II, B9.5V, G0V	8100, 10000, 6030
VB10	BS7235	A0V	9400

to be featureless and to be well described by a Rayleigh–Jeans energy distribution appropriate to their effective temperature. All observations were made in good conditions (better than 1-arcsec optical seeing) and the airmass difference between object and standard never exceeded 0.05. Thus we believe the spectra have excellent cancellation of atmospheric features. The observations were repeated on subsequent nights to check the cancellation of atmospheric features and the reproducibility was found to be better than 10 per cent peak-to-peak. An example is shown in Fig. 1 of GL406 (fully reduced) taken on different nights. Figs 2(a)–(c) show a spectral sequence ranking the M dwarfs based on the strength of water absorption features from 2.85 to 3.4 μm for each of the 150 line mm^{-1} grating positions.

3 CALCULATIONS OF *AB INITIO* WATER VAPOUR TRANSITIONS

At low temperatures water vapour absorption is very thoroughly studied. However few reliable data on hot water (above 1000 K) are available. Over the last decade a number of groups (e.g. Tennyson 1986; Spirko et al. 1985; Carter & Handy 1987) have developed techniques for calculating triatomic energy levels based on variational techniques. In particular, Sutcliffe & Tennyson (1986) have produced a ro-vibrational Hamiltonian which is exact within the constraints of the Born–Oppenheimer approximation (which decouples electronic from nuclear motion in a molecule) and the limitations of the electronic potential energy surface.

The Sutcliffe–Tennyson kinetic energy operator directly relates the Cartesian positions of the nuclei of a triatomic molecule to a set of internal coordinates comprising two radial coordinates and the included angle. Rotation of the molecule-fixed internal coordinates in the laboratory frame is carried out by the usual standard rotational matrices. The kinetic energy operator makes no a priori assumptions about ro-vibrational separation or equilibrium geometry. The method is described in Tennyson, Miller & Henderson (1993).

The ro-vibrational wavefunctions were calculated by using a suite of programs known as TRIATOM (Tennyson, Miller & Le Sueur 1993). The suite contains modules to calculate ro-vibrational transition frequencies and line strengths from dipole moment surfaces. Wavefunctions and energies were generated using the best then available (Fernley, Miller & Tennyson 1991) water potential due to Jensen (1989). Transition intensities were obtained using the program DIPOLE3 (Lynas Gray, Miller & Tennyson 1995; Tennyson, Henderson & Fulton 1995) and the dipole surfaces of Wattson & Rothman (1992).

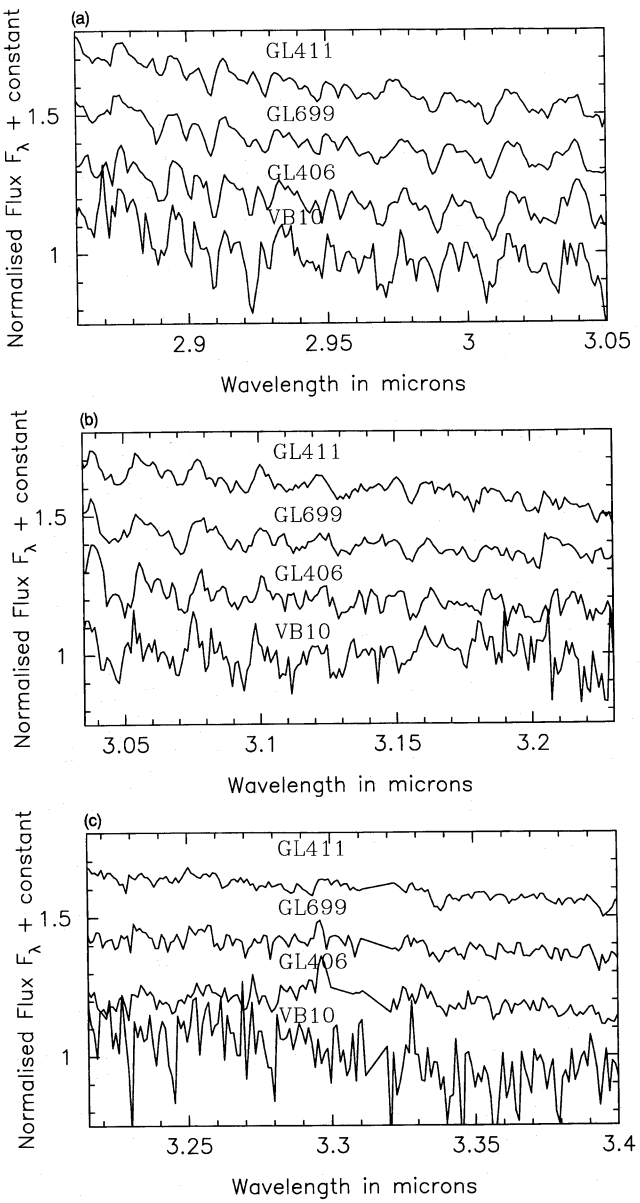

Figure 2. Spectral sequence for each grating position (a) at 2.94 μm, (b) at 3.12 μm and (c) at 3.30 μm. In plot (c) the region around 3.32 μm has been interpolated over in the region where the atmosphere is opaque due to a strong methane band. In each of the plots the observations are normalized to have the same mean value of one and then offset from one another by the addition of 0.2 to separate the spectra.

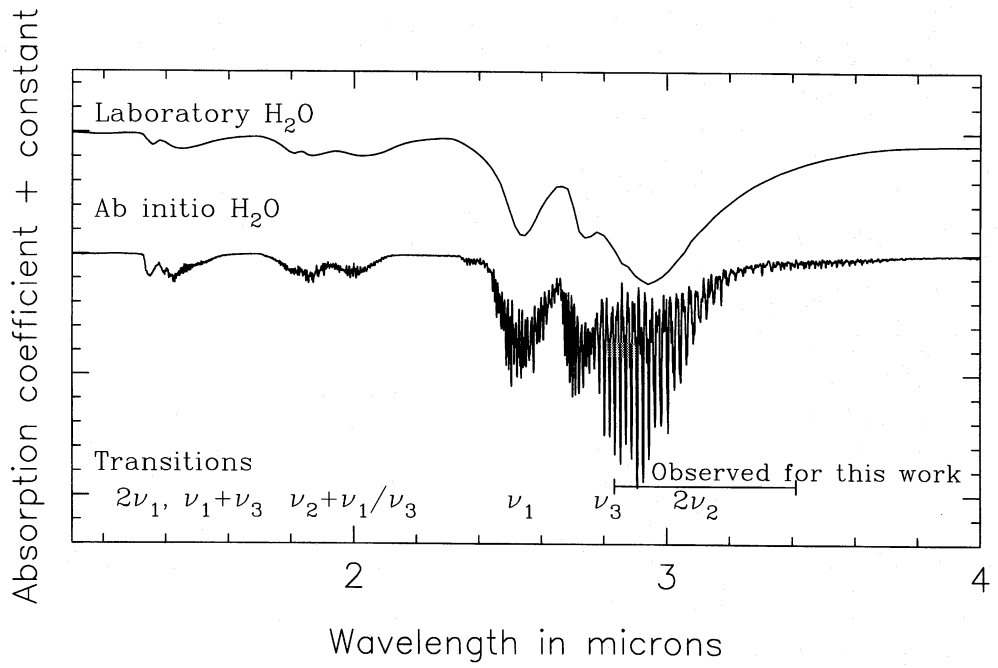

Figure 3. Comparison of Ludwig (1971) absorption coefficients for water vapour and those from the *ab initio* calculations at 3000 K. The band origins of the various features that make up the water vapour absorption coefficient are marked in the figure.

The calculation includes angular momentum states up to $J = 30$. All band origins up to 11 000 cm^{-1} above the ground state are included as well as many, but not all, higher ones. This energy cut-off is too low to include all the transitions expected at cool star temperatures, and shortward of around 2 μm the calculation does not give a good representation of stellar energy output (Allard et al. 1994). For longer wavelengths where higher energy transitions are relatively less important the calculation is expected to be much more reliable. This gives us confidence that the spectra observed for this study from 2.86 to 3.4 μm should be well represented by the calculation. The comparisons presented here extend the work of Miller et al. (1994) where the observed spectra were compared, without the use of a model atmosphere, with an earlier, less complete, generation of the calculation.

4 COMPARISON WITH OTHER WATER OPACITY DATASETS

Water was the first triatomic molecule to be included in a stellar atmosphere calculation (Tsuji 1967) and for 15 years remained the only one. The most frequently used source for water opacity is Ludwig (1971), whose data were obtained to assess the heating effect of radiation by hot water vapour in exhaust fumes from large rockets. Ludwig and co-workers measured the absorption of water in a flame between 1000 and 3000 K and hence tabulated absorption coefficients for water from 1.1 to 10.0 μm, albeit with low resolution. In Fig. 3 a comparison between Ludwig's experimental data and the *ab initio* data is shown. Water absorption from 2.85 to 3.20 μm, obtained for this work, can be seen as intrinsically very strong. The *ab initio* water plot has been made from a subset of 6000 strong transitions and scaled to appear similar in amplitude to the laboratory data, though its much higher resolution means Fig. 3 is not a proper comparison of the band intensities. For intercomparison of the *ab initio*, Ludwig and HITRAN (Rothman et al. 1992) datasets we refer to Schryber et al. (1995).

The Ludwig data have been widely used for the computation of cool star atmospheres, although other laboratory results, the *ab initio* line list used here and observations of cool stars themselves cast serious doubts on its accuracy. The Ludwig band strengths were derived by integrating the measured spectral emissivity of hot water vapour assuming that the fine structure of the spectrum is smeared out at high temperatures. Yamanouchi & Tanaka (1985) found that this assumption is not always valid and showed large differences for the strengths of the 1.1- and 1.4-μm bands between the Ludwig data and their work (in agreement with Goldstein 1964 and Burch & Gryvnak 1966). Schryber et al. (1995) find a similar mismatch with their calculation of the 1.9-μm band and suggest that Ludwig's results overestimate the absorption coefficient of water over the entire 1–2 μm region at higher temperatures.

Comparisons between synthetic and observed spectra for M dwarfs also indicate problems with the Ludwig dataset. The models of Mould (1976), Allard (1990), Ruan (1991), Tsuji (1994) and Brett (1995) which all use the Ludwig water opacities cannot simultaneously reproduce observed spectral energy distributions and absorption bands due to water vapour. For an effective temperature derived on the basis of spectral energy distribution the models all overestimate the importance of water vapour. This has prompted Brett (1995) to decrease the absorption coefficient arbitrarily for the Ludwig opacity data by a factor of three in a new set of cool dwarf models.

5 MODEL ATMOSPHERES

We use the model atmosphere code PHOENIX, version 4.9, to compute model atmospheres and synthetic spectra for cool

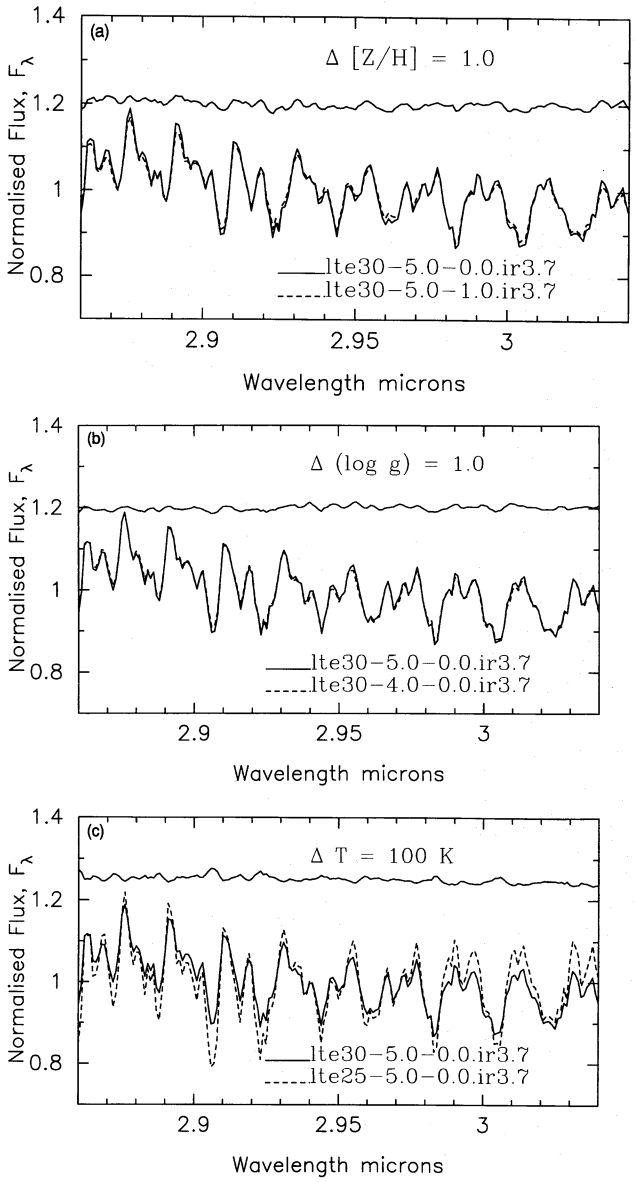

Figure 4. Comparisons between synthetic spectra showing the influence on the synthetic spectra of (a) varying metallicity by a factor of ten from solar abundance ([Z/H] = 0.0) to that of a metal-poor star ([Z/H] = −1.0), (b) varying surface gravity by a factor of 10 – the expected gravity difference between a young ~ 5-Myr, 0.2-$M_\odot$ star and one on the main sequence (Burrows et al. 1993), (c) varying effective temperature by 100 K (equivalent to about half a spectral type, e.g. M5 to M5.5).

dwarf stars. Its application to M dwarf atmospheres is described by Allard et al. (1994) and Allard & Hauschildt (1995). Here we draw attention to the important assumptions relevant for this study.

(i) Since the gravities are high (log g ~ 5), the atmospheres can be well approximated as plane-parallel.

(ii) The velocities of the convection cells are too small to be detected in low-resolution spectra and will have a negligible influence on the transfer of radiation, and so the effects of convective motion on line formation are neglected (Allard & Hauschildt 1995).

(iii) A treatment for molecular line broadening due to collisional processes, for example with H_2 and H^-, is not included. The line broadening for molecules is treated by altering ξ(molec), the isotropic micro-turbulent velocity for molecules caused by pressure and turbulent broadening, throughout the model structure. We investigate the effect of changing ξ(molec) in Section 6.1.

(iv) Non-local thermodynamical equilibrium (NLTE) effects are neglected. Although we are not aware of any research on their importance for transitions of hot water vapour, complex molecules have many pathways for any given population to thermalize and so NLTE effects probably play only a small role.

The major difference between models presented here and those in Allard et al. and Allard & Hauschildt is the inclusion of new data for TiO which has allowed it to be treated using the opacity sampling technique rather than the less reliable Just Overlapping Line Approximation (JOLA) technique (Tsuji 1994). Jorgensen (1994) has calculated a line list for TiO comprising 12 million lines. The new treatment of TiO has the effect of reducing the effective temperatures derived by comparisons with a previous generation of these model atmospheres (Kirkpatrick et al. 1993) around 1 μm by about 200 K (Jones et al. 1995). We thus consider the lack of molecular line lists for the other primary sources of opacity, VO and FeH, to be large uncertainties in the calculation of representative synthetic spectra for cool dwarf stars. However the inclusion of high-quality line lists for the TiO and H_2O means that we expect that the dominant opacity over much of the peak of the stellar energy distribution is well accounted for.

A small grid of synthetic spectra was calculated. We distinguish the different models using the notation lteTT–G.G–Z.Z.I.D, where lte = local thermodynamic equilibrium assuming ξ(LTE) = 2 km s^{-1}, TT = $T_{\rm eff}$/100, G.G = log g (surface gravity), Z.Z = [Z/H] (metallicity), where [Z] ≡ log $Z_{\rm star}$ − log $Z_\odot$ for any abundance quantity Z, and I.D = batch number (ir3.7 for ξ(molec) = 2 km s^{-1} and ir3a.7 for ξ(molec) = 50 km s^{-1}).

(i) For ξ(molec) = 2 km s^{-1}, models were calculated for $T_{\rm eff}$ = 2000, 2500, 3000, 3500 K, log g = 5.0, [Z/H] = 0.0 and $T_{\rm eff}$ = 3000 K, log g = 4.0, [Z/H] = 0.0 and $T_{\rm eff}$ = 3000 K, log g = 5.0, [Z/H] = −1.0.

(ii) For ξ(molec) = 50 km s^{-1} models were calculated for $T_{\rm eff}$ = 3000, 3500 K, log g = 5.0 and [Z/H] = 0.0.

Fig. 4 shows comparisons with models of different effective temperature, metallicity and gravity over a similar wavelength range to the observations. These are discussed in Section 6.2.

6 SPECTRAL ANALYSIS

The models were calculated at a resolution of 5 × 10^{-5} μm and were transformed to the instrumental resolution by smoothing with a block function to mimic the effect of being detected by the square pixels used by the infrared detector of CGS4 and resampling to the same oversampling (×3) as used for the observations. This was performed using routines within the KAPPA (Currie 1992) and SPECDRE (Meyerdierks 1993b) packages.

6.1 Line broadening

Detailed line profiles can be modelled for atomic lines because their damping constants are known, but they are not known for molecular transitions. Atomic lines computed with Voigt profiles and Van der Waals pressure broadening give an averaged full width half maximum of around 50 km s^{-1}. Initially this broadening was used to simulate the line broadening for water vapour transitions by setting ξ(molec) = 50 km s^{-1}. Although the 'true' microturbulence is expected to be close to 2 km s^{-1} (the speed of sound is 6–8 km s^{-1}) with this generation of models, setting ξ(molec) = 50 km s^{-1} is the most practical way of allowing for the pressure broadening of water vapour transitions. Models with ξ(molec) = 2 km s^{-1} (i.e. no pressure broadening) were also calculated. In Fig. 5, GL411 and GL406 are compared with 3500- and 3000-K models for ξ(molec) = 2 and 50 km s^{-1}. 11 The ξ(molec) = 50 km s^{-1} models predict enhanced strengths of water absorption bands across the entire spectral region, though particularly from 3.2 to 3.4 μm. To match the strengths of the water bands with the ξ(molec) = 50 km s^{-1} synthetic spectra it is necessary to increase the best-fitting effective temperatures by 200–800 K depending on the spectral region, effective temperature and adopted effective temperature scale. Doing so leads to a much poorer fit to the overall continua. The lack of agreement suggests that the damping constants of water (and therefore possibly all molecular lines), which are unknown, must be smaller than the damping constants of the average atomic lines. Alternatively water vapour lines form higher in the photosphere in regions of lower pressure. To test the latter hypothesis the model structure was investigated: for the 2500-K model it shows that the strongest water lines form in the outer parts of the atmospheres at gas pressures around 10^3 dyn cm^{-2}, the bulk of the water lines form around gas pressures of 5×10^4 dyn cm^{-2}, whereas weak atomic lines form much deeper, around gas pressures of 10^6 dyn cm^{-2}. The formation of water lines at relatively low pressures explains why microturbulent velocity provides sufficient line broadening to match the observed spectra.

Previous models of M dwarfs have generally assumed that the high densities prevalent in their atmospheres mean that molecular lines are smeared together by their large pressure broadening (JOLA, e.g. Tsuji 1994). However the water band strengths in Fig. 5 and new examination of the model structures indicate low pressure broadening and suggest that flux is escaping between the water vapour line transitions, undermining the use of the JOLA approximation for water vapour transitions in cool dwarf atmospheres. The reduction in opacity caused by water vapour lines forming at lower pressures leads to weaker band strengths. This result is likely to explain much of the apparent overestimate of molecular band strengths in synthetic spectra for M dwarfs (e.g., Persson, Aaronson & Frogel 1977; Reid & Gilmore 1984; Ruan 1991; Tinney et al. 1993; Brett 1995). In Fig. 6 we show 2500-K models for ξ(molec) = 2 and 50 km s^{-1}. The much weaker water bands seen around 1.4 and 1.9 μm in the ξ(molec) = 2 km s^{-1} model demonstrate how important this effect is for modelling the spectral energy distribution of M dwarfs across the peak of their energy distribution.

Low values for line broadening (modelled using the microturbulence parameter) are clearly most appropriate for water vapour lines. The following sections are based on models using ξ(molec) = 2 km s^{-1}, although this is not a proper physical approach to the damping problem and we do not yet know how the broadening varies between ξ(molec) = 2 and 50 km s^{-1}. The model atmosphere code is now being adapted so that the molecular broadening will be matched to the averaged atomic line broadening throughout the 50 layers between the 'standard' optical depths of $\tau_{std} = 10^{-10}$ and 10^2 in the model atmosphere. A computationally efficient method for achieving this is planned for the next generation of water vapour transitions.

6.2 Sensitivity to model parameters

Water vapour is well known to be extremely sensitive to colour temperature in M dwarfs (Baldwin, Frogel & Persson 1973). However, its dependence on metallicity and gravity differences has not been investigated. In Figs 4(a)–(c) the sensitivity of the synthetic spectra to changes in model parameters is examined. In each of (a), (b) and (c) one model parameter has been changed. In the lower part of each figure two models are normalized to have the same mean value and over plotted; in the upper part, the models have been divided by one another and the result offset by the addition of 0.25. The models were selected so that the differences in water band strength between them were similar. To reproduce a variation in water band absorption from a change in temperature, equivalent to those in metallicity and gravity, it was necessary to interpolate the coarse model grid in temperature. To mimic the effect of a 100-K change in effective temperature, 2500- and 3000-K synthetic spectra were divided by one another, multiplied by 0.2 and offset. A similar result was found when doing the same operation with the 3000- and 3500-K synthetic spectra.

In Fig. 4(a) a 3000-K, log g = 5.0 solar model (lte30-5.0-0.0.ir3.7) is compared to one with a tenth of solar metallicity. This comparison represents the probable extremes of metallicity of our sample objects (Jones et al. 1995) and indicates a small sensitivity to metallicity. In Fig. 4(b), 3000-K solar models with gravities of log g = 4.0 and 5.0, within the expected gravity difference for these objects, are compared. The plots indicate that water vapour features are not very sensitive to gravity effects. In contrast to the insensitivity of the spectra to metallicity and gravity, comparison of Fig. 4(c) with (a) and (b) indicates that a small change in effective temperature ($\sim$ 100 K) has a similar effect to that produced by a change of one dex in gravity or in metallicity. The differences between the models presented in Figs 4(a), (b) and (c) are smaller than the night-to-night differences between measurements across this spectral region (e.g. Fig. 1). With the observed sample, this study is not sensitive to differences in metallicity and gravity and so changes in water absorption strengths are treated as arising from differences of effective temperature between stars.

In Fig. 7 comparisons are made between the observed and synthetic spectra. We interpolate over the model grid to give a finer resolution in effective temperature and plot the best-fitting model for each observed spectrum. The intensities of the calculated ro-vibrational bands accord well with the observed ones, though the positions of the bands do not match so well. From the comparisons made by Fernley et al. (1991), the lowest 20 band origins are accurate to a standard deviation of $\sim$ 0.006 μm and higher vibrational states to better than 0.010 μm. These errors are a mixture of (a) systematic,

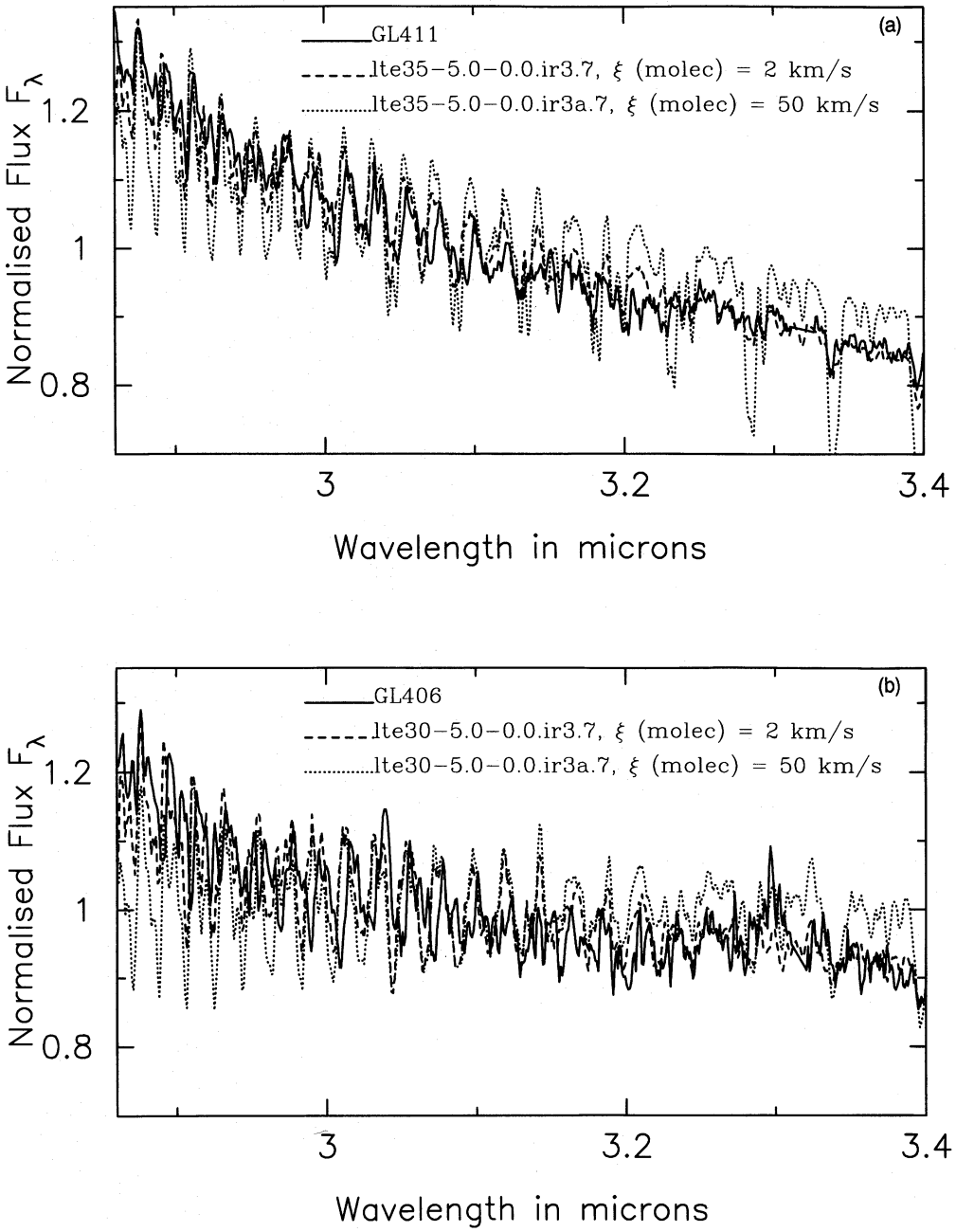

Figure 5. Comparison between observed and synthetic spectra from 2.86 to 3.4 μm using ξ(molec) = 2 and 50 km s^{-1} models: for (a) GL411 with 3500-K models and (b) GL406 with 3000-K models.

because Jensen's potential had a systematic error, (b) random, because the way Jensen determined the potential should leave a residual random error and (c) unknown, because only four excited bending states are known for water although the higher bends are at fairly low energies and are certainly important for these models. These errors on the *ab initio* calculation are considerably larger than the observational wavelength calibration error of $\sim$ 0.0006 μm (equivalent to a velocity of 180 km s^{-1}) or any wavelength shifts due to space velocity.

The wavelength differences between the models and the observations might arise from a simple expansion or contraction of the wavelength scale due to a systematic error in the potential surface used to compute the water vapour transitions. To examine this the observed and synthetic spectra were cross-correlated using the SCROSS routine within FIGARO (Meyerdierks 1993a). The spectra were cross-correlated with one another in 0.1-μm intervals every 0.05 μm from 2.86 to 3.4 μm and the standard deviations computed. The observed spectra have standard deviations of typically 0.0005 μm for the hotter stars as expected from the wavelength calibration errors, although the discrepancies with VB10 are much larger, $\sim$ 0.005 μm, due to its lower signal-to-noise ratio and markedly stronger water absorption bands. Comparison of the observations with their best-fitting synthetic spectra gives standard deviations around 0.015 μm and no evidence for a simple systematic wavelength shift between the models and observations.

Table 2. Comparison of the effective temperatures indicated by this study with those found by recent investigations.

Object	This Work ±200 K	Bessell ±50 K	Kirkpatrick et al. ±125 K	Tinney et al. ±110 K	Jones et al. ±160 K
GL411	3600	3500	>3500	3250	3471
GL699	3250	3250	-	3110	3095
GL406	3000	2800	3000	2580	2670
VB10	2750	2600	2875	2330	2506

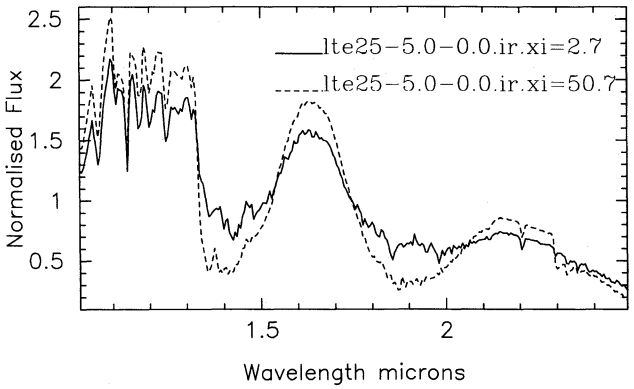

Figure 6. Comparison between synthetic spectra at 2500 K from 1.0 to 2.5 μm using ξ(molec) = 2 and 50 km s^{-1} models.

The wavelength discrepancies between synthetic and observed spectra are slightly larger than expected. We expect that this results from the lack of high-order transitions included in the water line list. Although the errors on the water line list are well characterized they do not account for the lack of higher order transitions, which means that there is an additional error term not included in the error estimate. As an example of the problems this can introduce, Grevesse & Sauval (1994) find that for the accurate modelling of line shifts and asymmetries for the CO molecule in the Sun it is essential to include transitions up to very high J levels.

6.3 Effective temperatures

Both models and observations indicate that water vapour transitions are not saturated but continue to increase with decreasing temperature as low as 2500 K. This is in agreement with Jones et al. (1994) where it was shown that the depths of the 1.4-, 1.9- and 2.6-μm water absorption features increase with decreasing effective temperature down to the coolest known dwarfs. Although the relatively short baseline of the observations presented here means that the underlying continuum is not very sensitive to temperature, the strengths of the water bands are sensitive, especially from 2.85 to 3.1 μm. In this region where the transitions are strongest we have interpolated over the model grid to estimate effective temperatures by overlaying a range of synthetic spectra on top of the observed spectra. The best-fitting by-eye values are given in Table 2 with values found by other recent studies of these objects. The error of 200 K reflects the uncertainty in finding a best-fitting model within the model grid but it does not reflect any errors in the model calculation. The apparent wavelength shifts between observed and model spectra due to the errors in the *ab initio* calculation prevent the spectra from matching exactly in wavelength; however, the intensities of the water band strengths are well determined and it is these which we use to estimate effective temperatures. Therefore, despite the lack of exact wavelength registration between the models and observations, we believe that such discrepancies will not lead to large systematic errors in effective temperature.

The effective temperatures for GL411 and GL699 are within the range of temperatures found by previous investigators, of whom Bessell (1991), Tinney et al. (1993) and Jones et al. (1994) used methods independent of the model atmosphere calculation. The effective temperatures for VB10 and GL406 are closest to those by Kirkpatrick et al. (1993). They also agree well with the temperatures determined by Bessell, agree less well with Jones et al. and differ most from those of Tinney et al. However it must be noted that the comparisons are only strictly appropriate for the effective temperatures derived by Kirkpatrick et al. The other investigations rely on an object's spectrum being close to a blackbody at the chosen wavelength points, and so find 'equivalent temperatures' (introduced and discussed by Tinney et al.) rather than the effective temperatures determined by this study.

The comparisons in Fig. 7 indicate that the molecular opacity in the observed spectral region is reasonably well modelled. However the models used for these comparisons do not have a complete inclusion of water opacity shortward of 2 μm (Allard et al. 1994), and so it seems unlikely that the model structure can be correct. Therefore we are not able to set a definitive effective temperature scale for M dwarfs. This must wait for the completion of the full water vapour calculation and a better understanding of molecular line broadening.

7 FUTURE WORK

The observational spectra presented here show good agreement with the models in terms both of predicted line strengths and line positions. From these comparisons and recent improvements in the computation, we are confident that a complete *ab initio* calculation can produce an accurate description for the transitions of hot water vapour. A new calculation of the water line list is underway with completion expected by early 1996. This list will include all energies levels up to 30 000 cm^{-1} with the aim that it will give an accurate representation of hot water vapour for transitions longward of ~0.2 μm with convergence to better than 0.1 cm^{-1}. We look forward to testing the match of this calculation included in PHOENIX to the spectra presented here and *ISO* measurements from 2.6 to 2.85 μm.

ACKNOWLEDGMENTS

We warmly thank John Fernley and Richard Jameson for inspiring this research. We are indebted to Andreas Schweitzer who played an important role in the recent improvements of

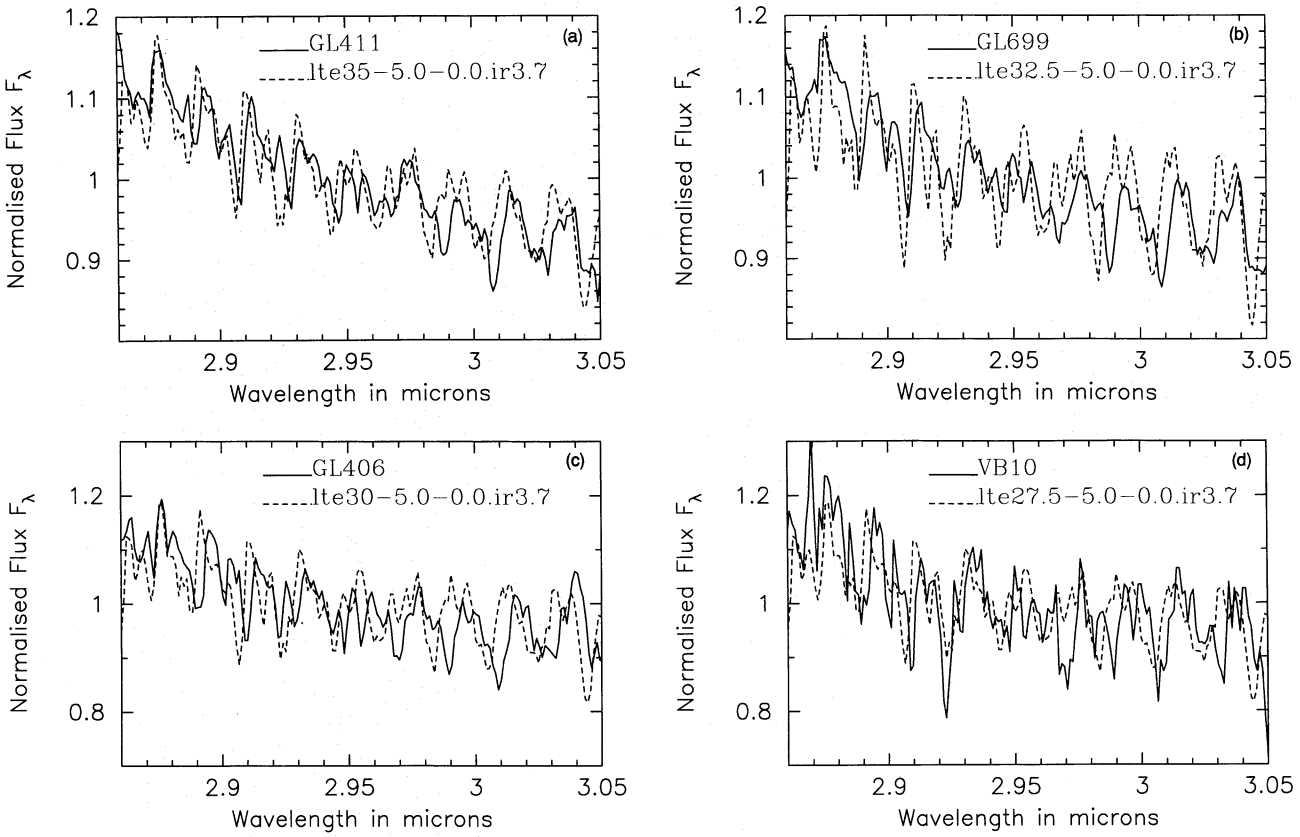

Figure 7. Comparisons of spectra with models: (a) GL411 and a 3500-K model, (b) GL699 and a 3250-K model, (c) GL406 and a 2800-K model, (d) VB10 and a 2500-K model. Models intermediate in effective temperature to those of the grid were created by linear interpolation.

PHOENIX. HRAJ acknowledges a SERC/PPARC studentship and latterly the DSS. PHH was supported by a NASA LTSA grant to Arizona State University. FA was supported in part by grants to G. Fontaine and F. Wesemael from FCAR (Quebec) and to G.F. Fahlman and H.B. Richer from NSERC. The development of PHOENIX's opacity database was sponsored by a grant from the AAS to FA. We acknowledge the SERC/PPARC for the use of computing facilities through STARLINK, for allocations of telescope time by PATT to use the UKIRT and for funding SM and JT. UKIRT is operated by the Royal Observatory Edinburgh from the Joint Astronomy Centre Hilo. Some of the calculations presented in this paper were performed on the Cray C90 of the San Diego Supercomputer Center. We thank them for a generous allocation of computer time.

REFERENCES

Allard F., 1990, PhD thesis, University of Heidelberg
Allard F., Hauschildt P., 1995, ApJ, 445, 433
Allard F., Hauschildt P., Miller S., Tennyson J., 1994, ApJ, 426, L39
Baldwin J.R., Frogel J.A., Persson S.E., 1973, ApJ, 184, 427
Bessell M., 1991, AJ, 101, 662
Brett J., 1995, A&A, 295, 736
Burch D.E., Gryvnak D.A., 1966, Absorption by H_2O between 5045–14485 cm^{-1}, Aeronutronic Report No. U-3704, Contract No. 3560(00)
Burrows A., Hubbard W.B., Saumon D., Lunine J.I., 1993, ApJ, 406, 158
Carter S., Handy N.C., 1987, J. Chem. Phys., 87, 4294
Currie M.J., 1992, Starlink User Note 95.8, Rutherford Appleton Laboratory
Fernley J.A., Miller S., Tennyson J., 1991, J. Molec. Spectrosc., 150, 597
Fowler A., 1904, Proc. R. Soc., 73, 219
Goldstein R., 1964, JQSRT, 4, 343
Grevesse N., Sauval A.J., 1994, in Jorgensen U.G., Thejl P., eds, Proc. IAU Colloq. 146, Springer-Verlag, Berlin, p.196
Hauschildt P.H., 1991, PhD thesis, University of Heidelberg
Hauschildt P.H., Starrfield S., Shore S.N., Gonzales-Riestra R., Sonneborn G., Allard F., 1994, AJ, 108, 1008
Hauschildt P.H., Starrfield S., Shore S.N., Allard F., Baron E., 1995, ApJ, 447, 829
Hoffleit D., Jaschek C., 1982, The Bright Star Catalogue. Yale University, New Haven
Jensen P., 1989, J. Mol. Spectrosc., 133, 438
Johnson H.L., 1966, ARA&A, 4, 193
Jones H.R.A., Longmore A.J., Jameson R.F., Mountain C.M., 1994, MNRAS, 267, 413
Jones H.R.A., Longmore A.J., Allard F., Hauschildt P., 1995, MNRAS, submitted
Jorgensen U., 1994, A&A, 284, 179
Kirkpatrick J.D., Kelly D.M., Rieke G.H., Liebert J., Allard F., Wehrse R., 1993, ApJ, 402, 643
Ludwig C.B., 1971, Appl. Opt., 10, 1057
Lynas Gray A.E., Miller S., Tennyson J., 1995, J. Molec. Spectrosc., 169, 458
Meyerdierks H., 1993a, Starlink User Note 86.9, Rutherford Appleton Laboratory
Meyerdierks H., 1993b, Starlink User Note 140.3, Rutherford Appleton Laboratory

Miller S., Tennyson J., Jones H.R.A., Longmore, A.J., 1994, in Jorgensen U.G., Thejl P., eds, Proc. IAU Colloq. 146, Springer-Verlag, Berlin, p.296
Mould J.R.M., 1976, A&A, 48, 443
Mountain C.M., Robertson D.J., Lee T.J., Wade R., 1990, Proc. SPIE, 1235, 3
Persson S.E., Aaronson M., Frogel J.A., 1977, AJ, 82, 729
Puxley P.J., Ramsay S.K., Beard S.M., 1992, in Grosbol P., ed., Proc. 4th ESO/ST-ECF data analysis workshop
Reid N., Gilmore G., 1984, MNRAS, 206, 19
Rothman L.S. et al., 1992, JSQRT, 48, 469
Ruan K., 1991, PhD thesis, National University of Australia
Schlosser W., Schmidt-Kaler T., Milone E.F., 1991, Challenges of astronomy: hands-on experiments for the sky and laboratory. Springer, New York
Schryber J.H., Miller S., Tennyson J., 1995, JSQRT, 53, 373
Spirko V., Jensen P., Bunder P.R., Cejchan A., 1985, J. Mol. Spectrosc., 112, 183
Sutcliffe B.T., Tennyson J., 1986, J. Mol. Phys., 53, 1053
Tennyson J., 1986, Comput. Phys. Rep., 4, 1
Tennyson J., Miller S., Henderson J.R., 1993, in Methods in Computational Chemistry, 4. Plenum, New York, p. 91
Tennyson J., Miller S., Le Sueur C.R., 1993, in Methods in Computer Phys. Comms., 75, p.339
Tennyson J., Henderson J.R., Fulton N.G., 1995, Comput. Phys. Commun., 86, 175
Tinney C.G., Mould J.R., Reid I.N., 1993, AJ, 105, 1045
Tsuji T., 1967, in Hack M., ed., Colloq. on Late-Type Stars. Astron. Obs. Trieste, p.260
Tsuji T., 1994, in Jorgensen U.G., Thejl P., eds, Proc. IAU Colloq. 146, Springer-Verlag, Berlin p.79
Wattson R.B., Rothman L.S., 1992, JQSRT, 48, 763
Yamanouchi T., Tanaka M., 1985, JQSRT, 34, 463

This paper has been produced using the Royal Astronomical Society/Blackwell Science LaTeX style file.